Proceedings of the 17th World Congress
The International Federation of Automatic Control
Seoul, Korea, July 6-11, 2008

Optimal Hybridization in Two Parallel Hybrid Electric Vehicles using Dynamic Programming ⋆

Olle Sundström [*,**] **Lino Guzzella** [*] **Patrik Soltic** [**]

[*] *Department of Mechanical and Process Engineering*
ETH Zurich 8092 Zurich, Switzerland
[**] *EMPA Material Science and Technology*
Überlandstrasse 129 8600 Dübendorf, Switzerland

Abstract: This study explores different hybridization ratios of two types of parallel hybrid electric vehicles, a torque assist parallel hybrid and a full parallel hybrid, with equal power-to-weight ratio. The powertrain consist of an internal combustion engine, an electric motor, and a NiMH battery. The different hybridization ratios are compared by their optimal fuel consumption for eight different drive cycles. The optimal fuel consumption is determined using dynamic programming for each of the different hybridization ratios. In the full parallel hybrid the engine and motor can be decoupled while in the torque assist hybrid the engine and motor are always mechanically connected. Results show that there are not only lower fuel consumption for the full hybrid but the need for hybridization is lower than in the torque assist hybrid for all eight cycles. The hybridization ratio where a full hybrid have the same fuel consumption as the optimal torque assist hybrid can differ as much as 51%.

1. INTRODUCTION

The interest for hybrid electric vehicles, i.e. vehicles including an internal combustion engine, an electric motor and a battery as power sources, is increasing among automotive manufacturers and researchers. Hybrid electric vehicles provide opportunities to reduce fuel consumption and hence reduce carbon dioxide emissions through brake energy recuperation, engine start-stop operation, and engine operating point shifting. This study will focus on a parallel hybrid electric vehicle where the electric motor and combustion engine are mechanically linked. Parallel hybrid vehicles can be divided into two separate classes: full parallel hybrids and torque assist hybrids. In a torque assist hybrid the motor and engine are always coupled while in a full hybrid the engine and motor can be decoupled. When dimensioning hybrid powertrains the problem always exist how to optimize the components without knowing how they will be used. In other words if the energy management strategy only utilizes the electric path rarely there will be a lower need for hybridization. If the energy management utilizes the electric path excessively there will be a greater need for hybridization.

There have been previous studies on dimensioning of the drive train components in a parallel hybrid electric vehicle like Lukic and Emadi [2004] and Holder and Gover [2006]. However, previous studies focusing on dimensioning uses a predefined energy management strategy, usually a rule-based strategy parameterized in different ways. When using a parameterized rule-based energy management strategy the different vehicle designs will benefit differently from the strategy and thus unavoidably giving a biased results, only valid for the specific parametrization. In Desbois-Renaudin et al. [2004] the authors study the energy losses for different hybridization ratios in a full parallel hybrid vehicle using optimal control methods. However the comparison between full and torque assist parallel hybrid is never made.

The aim of this study is to quantify the hybridization needs, i.e. the optimal dimensioning of the power train components, in two types of parallel hybrid electric vehicles and to exclude the influence of the control strategy on component sizing. The paper is structured as follows: Section 1.1 describes the method used to solve the design/control problem, Section 2 describes the parallel hybrid vehicle model and model scaling, Section 3 describes the dynamic programming algorithm, Section 4 shows the optimal hybridization of the parallel hybrid vehicle and finally Section 5 discusses the results and future work.

1.1 Method

To exclude the influence of the control strategy on component sizing an optimal control method is used. By using this method all different designs are evaluated based on their optimal performance and therefore compared on an equal basis. This method has been used to determine the effect of battery size on total energy losses in a fuel cell hybrid electric vehicle by Sundstroem and Stefanopoulou [2007]. Since the considered system is highly nonlinear and is valid under multiple complex constraints Bellman's dynamic programming algorithm (Bellman [1957]) is a suitable method to compute the optimal control input. The optimal hybridization is compared using eight different

⋆ This work is a part of the CLEVER project which is a common project of ETH, EMPA, Volkswagen and Bosch. The project is supported in part by the Swiss Federal Office of Energy, the Swiss Federal Office of Environment, and Novatlantis.

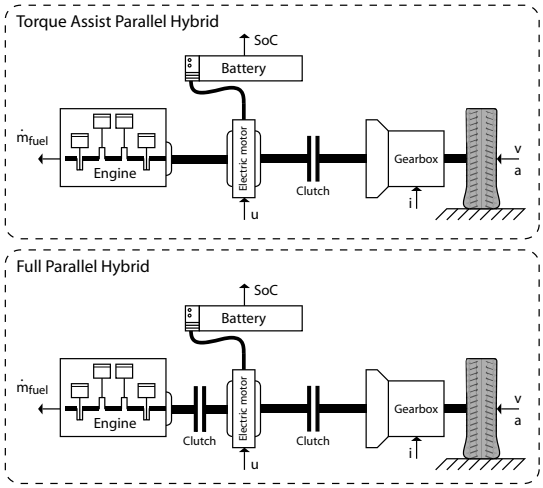

Fig. 1. Two types of parallel hybrid electric vehicle configurations: torque assist parallel hybrid (top) and full parallel hybrid (bottom).

drive cycles. The torque assist hybrid and the full hybrid configurations are shown in Fig. 1. Note that the full hybrid requires an electrically controlled clutch between the engine and motor and that the mechanically actuated clutch between the motor and gearbox in the full hybrid is not necessary if the gearbox is automated.

2. PARALLEL HYBRID VEHICLE MODEL

The parallel hybrid electric vehicle model is a quasi static, i.e. non causal, discrete model where the signals flow from the drive cycle through the power train one way. The modeling follows the theories in Guzzella and Sciarretta [2007]. The parallel hybrid electric vehicle model can be described as

$$x_{k+1} = f(x_k, u, v, a, i), \tag{1}$$

where x_k is the state of charge in the battery, u is the torque split factor (further described in Section 2.3), v is the vehicle speed, a is the vehicle acceleration and i is the gear number. Throughout this study a time step of one second has been used. The model is separated into the subsystems; vehicle, gearbox, internal combustion engine, electric motor, and a battery. The equations describing the subsystems and their scaling equations are shown in the following section. The model assumes no extra fuel consumption during starting of the combustion engine, isothermal conditions and no energy losses during gear shifting.

2.1 Vehicle

The vehicle model is based on a midsized vehicle with the mass of $m_0 = 1503$ kg equiped with a 1.6l internal combustion engine (totally $m_0 + m_{ice} = 1611$ kg). The total mass of the vehicle is

$$m_{veh} = m_0 + m_{ice} + m_{em} + m_{batt}, \tag{2}$$

where the engine mass m_{ice}, motor mass m_{em}, and battery mass m_{batt} are all depending on the specific component sizes.

The inputs to the vehicle model are the speed v_{veh} and the acceleration a_{veh} which is given by the drive cycle.

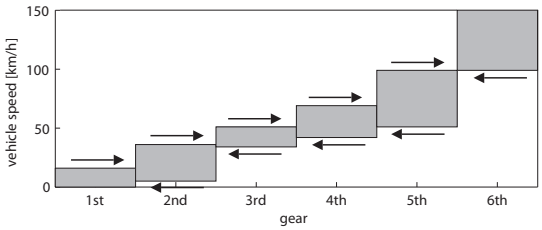

Fig. 2. Gear switching strategy when considering the manual gearbox.

The outputs of the model are wheel rotational speed ω_{veh}, wheel rotational acceleration $\Delta\omega_{veh}$, and the wheel torque T_{veh}. The outputs are determined from the inputs using the following equations

$$\omega_{veh} = v_{veh}/r_{wheel} \qquad \Delta\omega_{veh} = a_{veh}/r_{wheel}, \tag{3}$$

where r_{wheel} is the wheel radius and

$$T_{veh} = (F_f + F_a + F_i) \cdot r_{wheel}, \tag{4}$$

where the vehicle air drag force is

$$F_a = 0.5 \cdot \rho_{air} \cdot c_d \cdot A \cdot v_{veh}^2, \tag{5}$$

and the inertial force is

$$F_i = (m_{veh} + m_{rot}) \cdot a_{veh}, \tag{6}$$

with m_{rot} is the moment of inertia of the drivetrain converted into an equivalent mass. The friction force is

$$F_f = m_{veh} \cdot g \cdot (c_{r0} + c_{r1} \cdot v_{veh}^{c_{r2}}). \tag{7}$$

The friction coefficients c_{r0},c_{r1}, c_{r2}, and c_d have been identified using vehicle coastdown experiments. The vehicle model assumes no wheel slip.

2.2 Gearbox

The gearbox is a six gear manual transmission with the same gear ratios for all configurations. The inputs are the wheel speed, wheel acceleration, wheel torque, and gear number i. The outputs are the crankshaft rotational speed and acceleration together with the crankshaft torque. The gearbox efficiency is constant for all gears $\eta_{gb} = 0.95$ and thus the torque on the clutch side of the gearbox is

$$T_{gb} = \begin{cases} \dfrac{T_{veh}}{\eta_{gb} \cdot \gamma(i)} & T_{veh} \geq 0 \\ \dfrac{T_{veh} \cdot \eta_{gb}}{\gamma(i)} & T_{veh} < 0 \end{cases} \tag{8}$$

where $\gamma(i)$ is the gear ratio for each of the gears (including the final drive). The rotational speed of the crankshaft is

$$\omega_c = \gamma(i) \cdot \omega_{veh} \quad \text{and} \quad \Delta\omega_c = \gamma(\mathrm{i}) \cdot \Delta\omega_{\mathrm{veh}}. \tag{9}$$

The New European Drive Cycle (NEDC) includes a gear shifting strategy and since NEDC is used for rating of vehicles the given gear shifting strategy is used. The gear shifting strategy is, for all other drive cycles, given by a speed dependent shifting policy, shown in Fig. 2. When the vehicle speed exceeds the speed of the gray boxes in Fig. 2 there will be an upshift and when the speed is lower than the speed in the box then there will be a downshift. The gearbox model assumes no energy losses during gear shifting.

2.3 Torque Split

The torque split strategy in the hybrid vehicle, or more generally the energy management strategy (EMS), determines how the torque demand is split between the electric

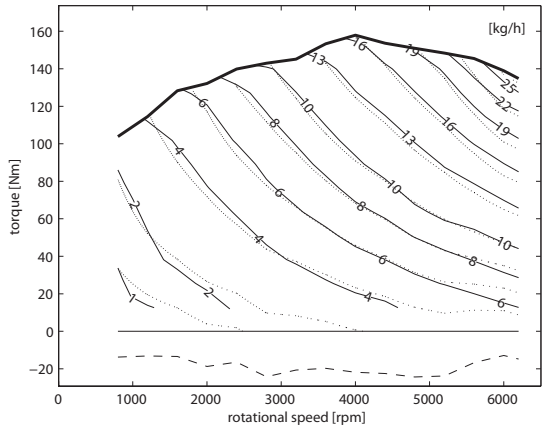

Fig. 3. Internal combustion engine fuel consumption map; measured (solid) and simulated (dotted). The drag mean effective torque is shown in dashed.

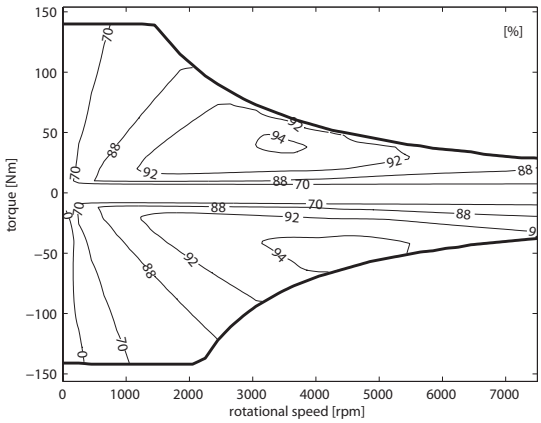

Fig. 4. Electric motor efficiency map with maximum and minimum motor torque.

motor and the internal combustion engine. The EMS refers to the control problem of determining the torque split factor at every time step. Let us define the torque split factor as the continuous variable $u \in [-1\ 1]$. The torque split factor can assign negative values (more torque is provided by the internal combustion engine than is demanded to recharge the battery with $u = -1$ being full recharge), zero $u = 0$ (torque is only provided using the internal combustion engine), positive values (torque is provided from both internal combustion engine and electric motor) and one $u = 1$ (all torque is provided by the electric motor or full brake energy recuperation).

The total torque demand required by the electric motor and the internal combustion engine will be different when considering a torque assist parallel hybrid compared to a full parallel hybrid. In the full hybrid the second clutch between the internal combustion engine and the electric motor allows the vehicle to run pure electric without dragging the internal combustion engine. A torque assist parallel hybrid on the other hand will always drag the internal combustion engine even when the vehicle is driving pure electrically since the motor and engine are always directly coupled. Therefore when considering the torque assist configuration the total torque demanded from combustion and/or the electric motor is

$$T_{dem} = T_{ice0} + T_{em0} + T_{gb}, \tag{10}$$

where T_{ice0} is the engine drag torque, T_{em0} is the electric motor drag torque, and T_{gb} is the demanded torque by the gearbox. In contrast when considering the full parallel hybrid the total demanded torque depends on the torque split factor as follows

$$T_{dem} = \begin{cases} T_{gb} + T_{em0} & u = 1 \text{ and } \mathrm{T_{em,max}} > \mathrm{T_{dem}} \\ T_{gb} + T_{em0} + T_{ice0} & \text{otherwise} \end{cases} \tag{11}$$

The electric motor torque demand and the internal combustion engine torque demand is determined using the total torque demand T_{dem}, the torque split factor u, the battery current limits, the motor torque limits, and the engine torque and speed limits.

2.4 Internal Combustion Engine

The internal combustion engine model is based on the Willans approximation, i.e. the brake mean effective pressure p_{bmep} is an affine function of the fuel mean effective pressure p_{fmep}

$$p_{bmep} \approx e(\omega_c) \cdot p_{fmep} - p_{bmep0}(\omega_c) \tag{12}$$

where $e(\omega_c)$ is the internal efficiency and $p_{bmep0}(\omega_c)$ is the drag mean effective pressure. The engine drag torque (including the inertial torque) is then given as

$$T_{ice0} = J_{ice} \cdot \Delta\omega_c + \frac{V_d \cdot p_{bmep0}(\omega_c)}{4 \cdot \pi} \tag{13}$$

with the inertia J_{ice} and the displacement V_d. The fuel consumption is calculated using

$$\Delta m_f = \frac{T_{ice} \cdot \omega_c}{e(\omega_c) \cdot Q_{lhv}}, \tag{14}$$

where Q_{lhv} is the lower heating value of gasoline. The rotational speed dependent variables $e(\omega_c)$ and $p_{me0}(\omega_c)$ have been fitted to measurement data from an engine dynamometer with a naturally aspirated 1.6 liter gasoline direct injection engine. A comparison between the measured and simulated fuel consumption map is shown in Fig. 3. Figure 3 shows that the model estimates the fuel consumption well. The mass of the internal combustion engine is approximated as

$$m_{ice} = V_d \cdot c_{dm/dV}, \tag{15}$$

with the constant $c_{dm/dV} = 67.6\ [kg/l]$.

2.5 Electric Motor

The model for the electric motor is generated based on detailed simulation data of a 24 kW motor. The motor drag torque is

$$T_{em0} = J_{em} \cdot \Delta\omega_c \tag{16}$$

with the motor inertia J_{em}. To determine the electric power needed from or supplied to the battery a map, $\Gamma(\omega, T)$, derived from the detailed simulations, is used

$$P_{em} = \Gamma(\omega_c, T_{em}) \tag{17}$$

The efficiency map of the 24 kW electric motor

$$\eta_{em}(\omega_c, T_{em}) = \begin{cases} \dfrac{T_{em} \cdot \omega_c}{\Gamma(\omega_c, T_{em})} & T_{em} \geq 0 \\ \dfrac{\Gamma(\omega_c, T_{em})}{T_{em} \cdot \omega_c} & T_{em} < 0 \end{cases} \tag{18}$$

is shown in Fig. 4.

2.6 Battery

The battery pack consists of multiple modules in parallel and in series which are each modeled as a voltage source in series with a resistance. The battery model is based on an ADVISOR model of a 6.5 Ah NiMH battery. The battery input/output power is the total power supplied to (or by) the electric motor $P_{em,tot}$

$$P_{em,tot} = P_{em} + P_{aux} \tag{19}$$

where $P_{aux} = 350$ W is a constant auxiliary power demand by the . The battery current I_{batt} is calculated using

$$I_{batt}(P_{em,tot}) = \frac{V_{oc} - \sqrt{V_{oc}^2 - 4 \cdot R_{int} \cdot P_{em,tot}}}{2 \cdot R_{int}}, \tag{20}$$

where V_{oc} is the open circuit voltage of the battery and R_{int} is the battery's internal resistance. Both the open circuit voltage and the internal resistance are functions of the state of charge and the number of modules, and cells per module, used in the battery pack. The battery current is limited to, $I_{min} \leq I_{batt} \leq I_{max}$, where I_{min} and I_{max} depends on the capacity of the battery. The battery's state of charge (SoC) x_k is calculated using

$$x_{k+1} = \frac{-I_{batt}\ \eta_{batt}(I_{batt})}{3600 \cdot Q_{batt}} + x_k \tag{21}$$

where η_{batt} is the battery charging efficiency

$$\eta_{batt}(I_{batt}) = \begin{cases} 1.0 & I_{batt} \geq 0 \\ 0.9 & I_{batt} < 0, \end{cases} \tag{22}$$

and Q_{batt} is the battery capacity.

2.7 Model Scaling

The internal combustion engine, electric motor and battery models have to be scaled to allow for different hybridization ratios. The combustion engine model is scaled using the displacement volume V_d according to the equations in Section 2.4. The stroke-to-bore ratio and the mean piston speed have been kept constant for all engine sizes. In the electric motor model the maximum torque and efficiency have been scaled using a linear dependency on the rated maximum power. The mass and inertia of the motor have also been scaled using a linear relationship of the maximum power. In the battery model the open circuit voltage has been kept constant while the internal resistance and battery mass have been scaled based on the battery capacity. The battery maximum power is given by the maximum power of the electric motor and hence the maximum battery current and therefore the battery capacity.

The total maximum power of the vehicle $P_{tot,max}$ is the maximum power of the two power sources together

$$P_{tot,max} = \max_{\omega} \left(T_{ice,max}(\omega) + T_{em,max}(\omega)\right) \cdot \omega, \tag{23}$$

where $T_{ice,max}$ is the maximum torque of the engine and $T_{em,max}$ is the maximum torque of the electric motor. Let

$$\omega^o = \arg\max_{\omega} \left(T_{ice,max}(\omega) + T_{em,max}(\omega)\right) \cdot \omega, \tag{24}$$

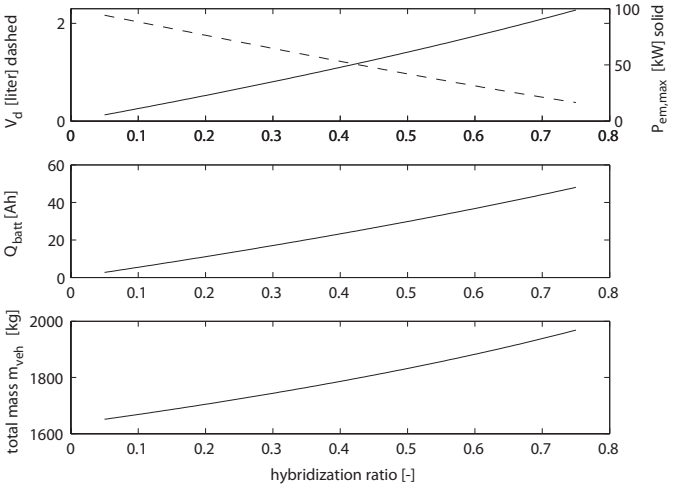

Fig. 5. Engine displacement, motor maximum power, vehicle total mass, and battery capacity with changing hybridization ratio.

then the hybridization ratio is defined as

$$HR = \frac{P_{em,max}(\omega^o)}{P_{tot,max}} \tag{25}$$

When optimizing the hybridization ratio in the vehicle it is only interesting to compare ratios with similar performance. Performance can be defined in several ways such as time from 0-100 km/h, top speed and gradability. The time from 0-100 km/h is strongly related to the maximum power-to-weight ratio which include both engine and electric motor size. This study therefore compare different hybridization ratios with equivalent maximum power-to-weight ratio (≈ 67 W/kg). The different vehicle characteristics are shown in Fig. 5. Since the total vehicle mass is increasing with increasing hybridization the total maximum power also increases to maintain equal power-to-weight ratio.

3. DYNAMIC PROGRAMMING

Let the discrete model (1) be reduced to

$$x_{k+1} = f_k(x_k, u_k), \qquad k = 0, 1, ..., N-1 \tag{26}$$

with the state of charge $x_k \in S_k$ and the torque split factor $u_k \in C_k$. Furthermore assume that the drive cycle is known in advance and that the particular driving speed, acceleration and gear number at instance k are included in the model function f hence the subscript k.

Let then $\pi = \{\mu_0, \mu_1, ...\mu_{N-1}\}$ be a torque split strategy for the particular drive cycle and vehicle model. Further let the cost of using π with the initial state $x(0) = x_0$ be

$$J_\pi(x_0) = g_N(x_N) + \sum_{k=0}^{N-1} g_k(x_k, \mu_k(x_k)), \tag{27}$$

with $g_N(x_N)$ being the final cost which is zero for $SoC(N) = SoC(0) = 0.6$ and infinite otherwise, thus forcing a charge sustaining solution. The final and initial state of charge has been chosen 0.6 since this is between the limits of the battery. Changing the final and initial value would have a small effect on the overall fuel consumption, if the state of charge trajectory is within the boundaries of the battery, since the state of charge only have a small

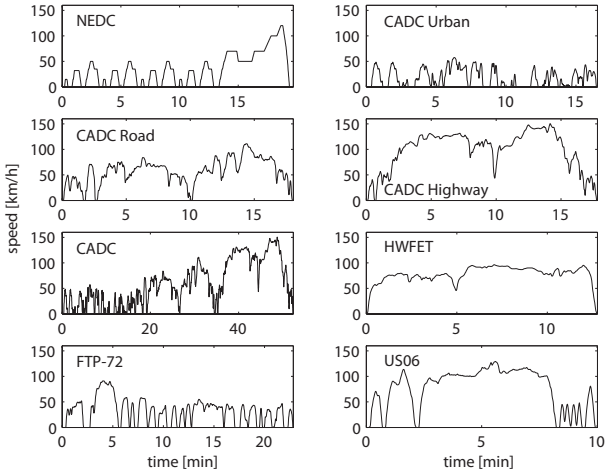

Fig. 6. The drive cycle speed profiles used.

effect on battery characteristics. The cost function g_k is the fuel consumption of the combustion engine, see equation (14). The optimal trajectory π^o is the trajectory that minimizes J_π

$$J^o(x_0) = \min_{\pi \in \Pi} J_\pi(x_0) \tag{28}$$

Bellmans principle of optimality (Bellman [1957]) states that an optimal input trajectory for a discrete decision problem going from $t = 0$ to $t = T$ is also optimal for the subproblem going from $t = n$ to $t = T$. Based on the principle of optimality, dynamic programming is the algorithm, which proceeds backward in time from $N - 1$ to 0,

(1) End cost calculation step

$$J_N(x_N) = g_N(x_N) \tag{29}$$

(2) Intermediate calculation step

$$J_k(x_k) = \min_{u_k \in U_k(x_k)} g_k(x_k, u_k) + J_{k+1}(f_k(x_k, u_k)) \tag{30}$$

The optimal torque split factor is given by the argument that minimizes the right side of equation (30) for each x_k and k. Before using the dynamic programming algorithm the input space $C = [-1\ 1]$ and state space $S = [0.4\ 0.7]$ must be limited and discretized. Further the state of charge upper and lower boundaries have been precalculated before using the dynamic programming algorithm. The state of charge boundaries are important to know exactly because the optimal state of charge trajectory will, in the end of the drive cycles, tangent the boundaries since it is optimal to recuperate as much as possible during the final braking phase of the drive cycle. Further the dynamic programming optimizations have been implemented in a way that allows the utilization of a computer cluster and distributed calculations.

4. RESULTS

The drive cycles used to compare different hybridization ratios for the two configurations are shown in Fig. 6. When using dynamic programming on the torque split strategy problem, for a particular drive cycle and hybridization ratio, the results is an optimal torque split map over time and state of charge. To get the optimal state trajectory and the minimum CO_2 emission, the optimal torque split

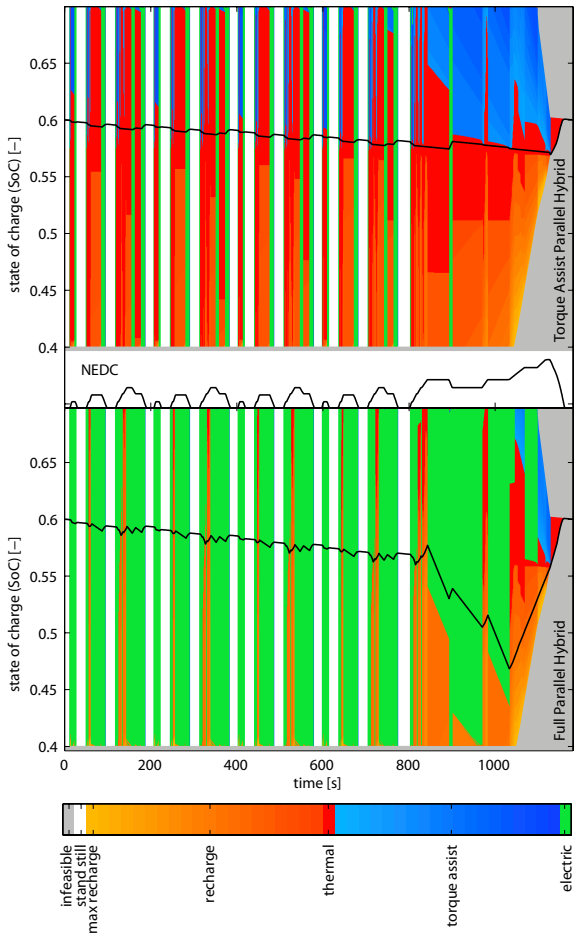

Fig. 7. The optimal input map for the torque assist hybrid (top) and the full hybrid (bottom) with 20% hybridization ratio driving the NEDC (middle) and the optimal state of charge trajectory (black).

map is used to determine the torque split during a forward simulation of the vehicle for the same drive cycle. Figure 7 shows the optimal input map and the optimal state of charge trajectory (when starting in $x_0 = 0.6$) for the NEDC of a torque assist hybrid and a full hybrid with 20% hybridization ratio. Note that the optimal strategy is very different in the two types of hybrids. In the full hybrid there are long periods of pure electric driving (green) while in the torque assist hybrid the engine and motor both supplies power (blue). The only time the torque assist hybrid is using the motor solely is during the braking and starting phases. The actual optimal input trajectory is the torque split (color) exactly on the state of charge trajectory (black line) in Fig. 7. The resulting CO_2 emission for the 20% torque assist hybrid is 161.5 g/km and for a full hybrid with the same hybridization is 118.7 g/km which is approximately 27% less.

In order to see the influence of hybridization on CO_2 emissions the torque split problem is solved using dynamic programming for hybridization ratios ranging from 5% to 75% with a step of 0.5%. The resulting CO_2 emissions for the eight different drive cycles are shown in Fig. 8. The resulting optimal hybridization ratios and comparisons are summarized in Table 1. Since the step in hybridization is 2.5% the numbers in Table 1 are only a rough estimate.

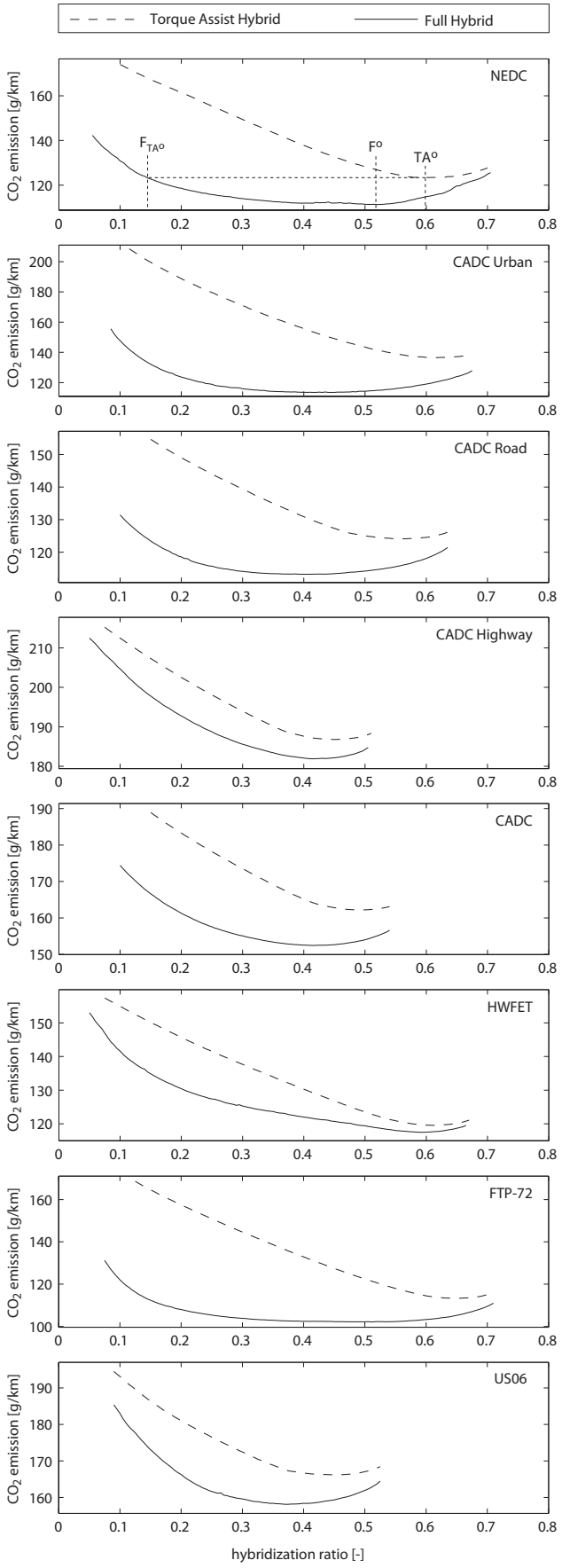

Fig. 8. Carbon dioxide emissions for the torque assist hybrid (dashed) and the full hybrid (solid)

Table 1. Optimal hybridization ratio for the torque assist hybrid (TA^o), the full hybrid (F^o) and the difference ($TA^o - F^o$). The hybridization ratio where the full hybrid has the same CO_2 emission as the optimum of the torque assist hybrid (F_{TA^o}) and the difference ($TA^o - F_{TA^o}$)

	Hybridization Ratio (%)				
Cycle	TA^o	F^o	$TA^o - F^o$	F_{TA^o}	$TA^o - F_{TA^o}$
NEDC	59.5	52	7.5	14.4	45.1
CADC U.	62	45	17	13.3	48.7
CADC R.	56	40	16	14.5	41.5
CADC H.	45	41.5	3.5	27.9	17.1
CADC	49	41.5	7.5	19.1	29.9
HWFET	61.5	59.5	2	49.2	12.3
FTP-72	65	51	14	14.2	50.8
US06	45.5	37	8.5	20.1	25.4

5. CONCLUSION AND FUTURE WORK

We can conclude that for all eight drive cycles the optimal hybridization is lower in a full parallel hybrid than in a torque assist parallel hybrid. The difference in hybridization ratio between the optimal torque assist hybrid and the full hybrid that has the same fuel consumption and CO_2 emission can be as high as $\approx 51\%$ (see FTP-72 in Table 1 and Fig. 8). What is more, the difference in CO_2 emissions between the torque assist hybrid and the full hybrid increases with decreasing hybridization ratio. For a 20% hybrid driving the NEDC there is a 27% reduction of the fuel consumption when including an extra electronically controlled clutch. Since this study does not consider any energy losses during clutching and during starting of the combustion engine, the results of the full parallel hybrid is optimistic. This study assumes a predefined gear switching strategy and fixed gear ratios therefore future work will investigate the gear switching strategy's and ratios' influence on the results. Future work also include an analysis of the phenomenons that explain why the hybridization requirements in a full hybrid is smaller than in a torque assist hybrid.

REFERENCES

R. E. Bellman. *Dynamic Programming*. Princeton University Press, 1957.

M. Desbois-Renaudin, R. Trigui, and J. Scordia. Hybrid powertrain sizing and potential consumption gains. In *Vehicle Power and Propulsion Conference, 2004. VPPC '04. IEEE*, pages 1–8, 2004. Paris.

L. Guzzella and A. Sciarretta. *Vehicle Propulsion Systems, Introduction to Modeling and Optimization, Second Edition*. Springer, 2007.

C. Holder and J. Gover. Optimizing the hybridization factor for a parallel hybrid electric small car. In *Vehicle Power and Propulsion Conference, 2006. VPPC '06. IEEE*, pages 1–5, 2006. Windsor.

S. M. Lukic and A. Emadi. Effects on drivetrain hybridization on fuel economy and dynamic performance of parallel hybrid electric vehicles. *IEEE Transactions on Vehicular Technology*, March 2004.

O. Sundstroem and A. Stefanopoulou. Optimum battery size for fuel cell hybrid electric vehicle, part 1. *ASME Journal of Fuel Cell Science and Technology*, May 2007.